Received: 2 December 2020 | Revised: 3 January 2021 | Accepted: 7 January 2021

DOI: 10.1002/ardp.202000455

FULL PAPER

ARCH PHARM DPhG
Archiv der Pharmazie

Design, synthesis, molecular docking, and some metabolic enzyme inhibition properties of novel quinazolinone derivatives

Feyzi S. Tokalı[1] | Parham Taslimi[2] | İbrahim H. Demircioğlu[3] | Muhammet Karaman[4] | Mehmet S. Gültekin[3] | Kıvılcım Şendil[5] | İlhami Gülçin[3]

[1]Department of Material and Material Processing Technologies, Kars Vocational School, Kafkas University, Kars, Turkey

[2]Department of Biotechnology, Faculty of Science, Bartin University, Bartin, Turkey

[3]Department of Chemistry, Faculty of Science, Atatürk University, Erzurum, Turkey

[4]Department of Molecular Biology and Genetics, Faculty of Arts and Sciences, Kilis 7 Aralik University, Kilis, Turkey

[5]Department of Chemistry, Faculty of Arts and Sciences, Kafkas University, Kars, Turkey

Correspondence
Feyzi S. Tokalı, Department of Material and Material Processing Technologies, Kars Vocational School, Kafkas University, 36100 Kars, Turkey.
Email: feyzitokali@gmail.com and feyzitokali@kafkas.edu.tr

Abstract

3-Amino-2-ethylquinazolin-4(3*H*)-one (**3**) was synthesized in two steps from the reaction of amide (**2**), which was obtained from the treatment of methyl anthranilate (**1**) with propionyl chloride, with hydrazine. From the reaction of 3-amino-2-ethylquinazolin-4(3*H*)-one (**3**) with various aromatic aldehydes, novel benzylidenaminoquinazolin-4(3*H*)-one (**3a–n**) derivatives were synthesized. The structures of the novel molecules were characterized using infrared spectroscopy, nuclear magnetic resonance spectroscopy (^{1}H-NMR and ^{13}C-NMR), and high-resolution mass spectroscopy. The novel compounds were tested against some metabolic enzymes, including α-glucosidase (α-Glu), acetylcholinesterase (AChE), and human carbonic anhydrases I and II (hCA I and II). The novel compounds showed K_i values in the range of 244–988 nM for hCA I, 194–900 nM for hCA II, 30–156 nM for AChE, and 215–625 nM for α-Glu. The binding affinities of the most active compounds were calculated as −7.636, −6.972, −10.080, and −8.486 kcal/mol for hCA I, hCA II, AChE, and α-Glu enzymes, respectively. The aromatic ring of the quinazoline moiety plays a critical role in the inhibition of the enzymes.

KEYWORDS

3-aminoquinazolin-4(3*H*)-one, enzyme inhibition, metabolic enzymes, molecular docking, Schiff bases

1 | INTRODUCTION

Quinazolines and quinazolinone derivatives are molecules that represent an important class of heterocyclic compounds. This class of compounds that are known to be natural and synthetic derivatives has attracted the attention of many scientists due to their biological activities and many molecules belonging to this class of compounds have been synthesized in the past 30 years. Many studies concerning anticancer,[1–4] antitumor,[5,6] antimicrobial,[7–9] anti-inflammatory,[10] antifungal,[11] anticonvulsant,[12,13] and anti-HIV[14] properties of quinazoline and quinazolinone derivatives have been reported.

Carbonic anhydrases (CAs) are metalloenzymes widespread in nature, being encoded by at least eight genetic classes, which have been identified in organisms.[15,16] By catalyzing a crucial physiologic reaction, by which carbon dioxide is hydrated with the formation of a weak base (bicarbonate) and a strong acid (hydronium ions), these enzymes are involved in plenty of physiologic mechanisms, starting with pH regulation and ending with metabolism.[17,18] Thus, CAs and their inhibitors are drugs having pharmacological applications in many fields. For example, CA II isoenzyme is the most physiologically relevant isoform and is implicated in diseases like glaucoma (such as CA XII), cerebral edema, and epilepsy.[19–21]

Alzheimer's disease (AD), characterized by memory loss, language, and cognitive impairment, and severe behavioral abnormalities, is an age-related and progressive neurodegenerative disorder.[22,23] At present, approximately 46 million people worldwide suffer from dementia, which is expected to reach 131.5 million by 2050. Due to the complex and unidentified etiology, many factors are perceived to be related to the occurrence and development of AD, including acetylcholine (ACh) decline, β-amyloid (Aβ) deposits, dyshomeostasis of biometals, oxidative stress, and hyperphosphorylated τ-protein. Current clinical drugs for AD treatment can only temporarily and modestly improve cognitive function, but they cannot significantly modify the course and the final outcome of the disease.[24–26] Thus, there is an urgent need for new AD therapy strategies. ACh is one of the key neurotransmitters in the human body, acting as a chemical messenger for conveying signals through the nerve synapse. The impairment of central cholinergic transmission has been related to a plethora of diseases, including AD, Parkinson's disease, schizophrenia, and epilepsy. In both the central and peripheral nervous systems, the termination of impulse transmission occurs via rapid ACh hydrolysis by the enzyme acetylcholinesterase (AChE). AChE converts ACh into choline and acetic acid, thus causing the return of a cholinergic neuron to its resting state.[27–30]

α-Glucosidases (α-Glu) (E.C.3.2.1.20) are glycoside hydrolase enzymes that play a vital role in the digestion of carbohydrates. These enzymes also help in the processing of cell surface oligosaccharides, which have crucial roles in cell-to-cell recognition during several infections, metastasis, and immune responses.[31] Thus, agents possessing the ability to inhibit the α-Glu enzyme can be used as therapeutics against many carbohydrate-linked diseases like diabetes mellitus (DM) type 2.[32–34]

This study was aimed at the synthesis of novel Schiff bases derived from 3-amino-2-ethylquinazolin-4(3*H*)-one and investigation of their effects on some metabolic enzymes.

2 | RESULTS AND DISCUSSION

2.1 | Chemistry

3-Amino-2-ethylquinazolin-4(3*H*)-one (**3**) was synthesized in two steps, with a good yield (87%), from the reaction of amide (**2**), which was obtained from the treatment of methyl anthranilate (**1**) with propionyl chloride, with hydrazine. In the second step, 3-amino-2-ethylquinazolin-4(3*H*)-one was treated with various aromatic aldehydes in acetic acid and the target compounds (**3a–n**) (Figure 1) were obtained with good yields (85–93%). The structures of the novel molecules were characterized using Infrared spectroscopy (IR), nuclear magnetic resonance spectroscopy (^{1}H-NMR and ^{13}C-NMR), and high-resolution mass spectroscopy (HRMS).

In the IR spectra of the compounds (**3a–n**), C=O and CH=N stretching bands were observed at 1699–1632 and 1607–1569 cm^{-1}, respectively. C=O and CH=N stretching bands are the characteristic bands of the compounds and are compatible with the structures.

In the ^{1}H NMR spectra of the compounds (**3a–n**), peaks of N=CH protons were observed as a singlet at δ 9.89–8.74 ppm. Aromatic

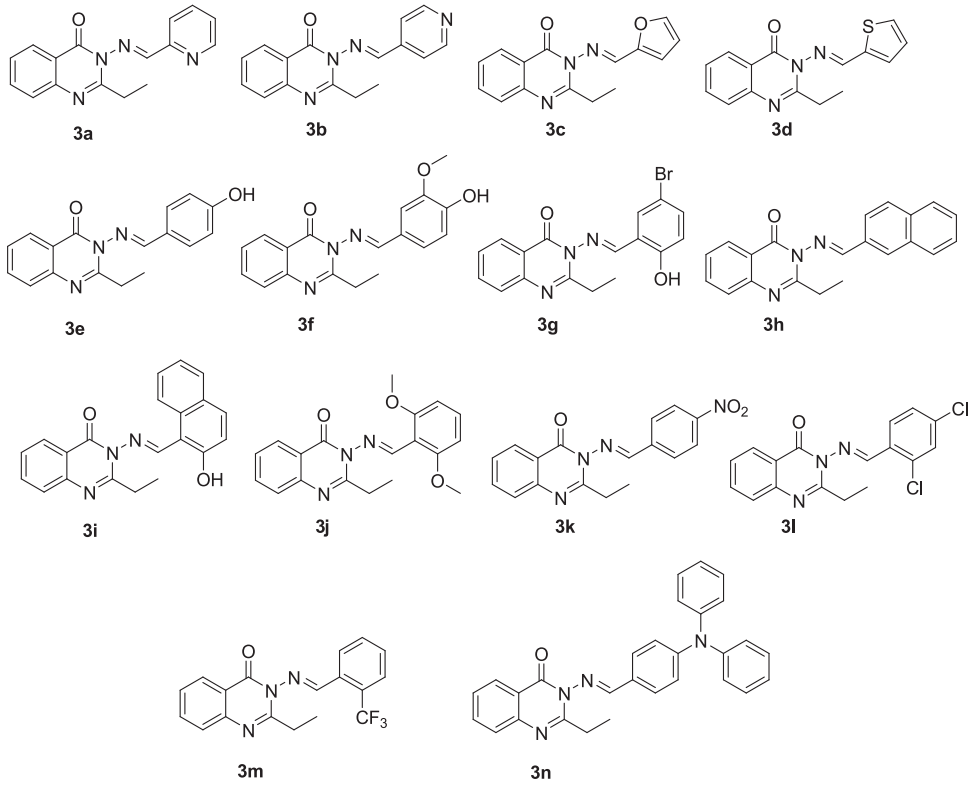

FIGURE 1 Structures of compounds **3a–n**

protons were observed at δ 8.80–6.61 ppm as singlet, doublet, triplet, and multiplet, relative to their chemical environment. Peaks of $\underline{CH_2}CH_3$ and $CH_2\underline{CH_3}$ protons were seen as a quartet at δ 3.08–2.83 and as a triplet at δ 1.44–1.25 ppm, respectively. Phenolic protons of compounds **3e**, **3g**, and **3i** were observed as a singlet at δ 10.39, 10.82, and 12.30 ppm, respectively. Chemical shifts, integrations, and splits are fully compatible with structures.

In the ^{13}C NMR spectra of the new compounds, peaks of C=O carbons were observed at δ 166.6–158.8 ppm. Peaks of CH=N carbons of the quinazoline ring and CH=N carbons of benzylidenamino moieties were seen at δ 159.3–157.6 ppm and δ 147.2–146.0 ppm, respectively. Peaks of aromatic carbons were observed at δ 169.5–107.3 ppm. For compounds **3f** and **3j**, peaks of OCH_3 carbons were seen at δ 56.2–55.9 ppm. Peaks of $\underline{CH_2}CH_3$ and $CH_2\underline{CH_3}$ carbons were observed at δ 28.7–27.4 and δ 11.2–10.4 ppm, respectively.

Finally, in the HRMS spectra of the target compounds, the found M+1 molecular ion values are compatible with the calculated M+1 molecular ion values.

The spectral data of IR, ^1H-NMR, ^{13}C-NMR, and HRMS are fully compatible with the structures of the molecules.

2.2 | Enzyme inhibition results

The enzyme inhibitory effects of all the novel benzylidenaminoquinazoline-4(3*H*)-ones (**3a–n**) were evaluated against hCA I, hCA II (cytosolic) as well as AChE, and α-Glu using the former assays. The inhibitory activities were compared with acetazolamide for cytosolic hCA I and hCA II isoenzymes, tacrine (TAC) for AChE, and acarbose for the α-Glu enzyme, and the results are presented in Table 1.

CA inhibitors (CAIs) were used in therapy as diuretics in the 1950s; however, nowadays, they are not only used for such applications, but also as antiepileptics, antiglaucoma agents, and antiobesity drugs.[35,36] Furthermore, some CAIs are in several phases of clinical development for the management of metastatic and hypoxic tumors. It should be also noted that, recently, some types of CAIs showed promising activity for the management of conditions like cerebral ischemia, arthritis, neuropathic pain, idiopathic intracranial hypertension, and some neurodegenerative disturbances.[37] Additionally, the CA activators have pharmacological applications in memory treatment and in the modulation of emotional memory, which opens the possibility to apply them in areas with few therapeutic options at this moment, such as posttraumatic stress, generalized anxiety, phobias, and obsessive-compulsive disorders.[38] The target compounds (**3a–n**) were screened for their potential against the two cytosolic hCA isoforms, namely hCA I and hCA II, using acetazolamide (AZA) as a standard and clinical drug. The novel compounds have shown significant inhibition at the nanomolar level against the cytosolic isoform hCA I, which exists in erythrocytes at a high level. It is well known that lower K_i values indicate a strong inhibitor affinity of inhibitors to enzymes. The inhibition types and K_i constants of novel molecules were obtained from Lineweaver–Burk graphs, as described previously. Compounds **3a–n** showed nanomolar inhibition levels against hCA I with K_i values between 244 ± 25 and 988 ± 77 nM (Table 1). Also, compound **3g** had the best inhibition effect toward hCA I (K_i: 244 ± 25 nM), compared with the standard compound AZA that exhibits a K_i value of 1137 ± 115 nM for cytosolic hCA I isoenzyme ($K_{i\text{-AZA}}/K_{i\text{-}\mathbf{3g}}$: 4.66). All undesirable side effects form a result of its nonspecific CAs inhibition. The results clearly displayed that novel compounds had an effective inhibition profile than that of AZA against cytosolic hCA I isoform (Table 1). Regarding the inhibition effects against hCA II, the tested molecules (**3a–n**) demonstrated a similar inhibition potency with K_i values ranging from 194 ± 29 to 900 ± 83 nM. However, AZA that is used to treat glaucoma and some other diseases had a K_i value of 1210 ± 204 nM against hCA II. As can be seen in Table 1, similar to CA I inhibition, compound **3l** had the greatest selectivity against hCA II isoenzyme. The activity of compound **3l** is promising. In other words, it possessed a maximum inhibition profile and can be used for the treatment of glaucoma after advanced examinations ($K_{i\text{-AZA}}/K_{i\text{-}\mathbf{3l}}$: 6.24) (Table 1). Inhibition types of the hCA I and hCA II were determined as noncompetitive.

AChE inhibitors mainly include carbamates and organophosphorus compounds. Carbamates are used as insecticides (e.g., aldicarb, carbofuran, carbaryl, ethienocarb, and fenobucarb) and as medications (e.g., neostigmine, rivastigmine, physostigmine, and pyridostigmine), which serve to elevate the cholinergic tone in pathologies including AD, myasthenia gravis, and glaucoma.[39,40] In recent years, the development of new AChE inhibitors has become a research hotspot. Novel compounds **3a–n** had K_i values ranging from 30 ± 6 to 156 ± 17 nM for AChE (Table 1). However, TAC had a K_i value of 167 ± 24 nM against the indicated AChE enzyme. It could be seen from the table that all compounds demonstrated marked inhibitory effects against both cholinesterases with K_i values in the subnanomolar range; however, compound **3m** showed a perfect inhibition effect against AChE ($K_{i\text{-TAC}}/K_{i\text{-}\mathbf{3m}}$: 5.57) (Table 1). The inhibition type of the AChE was determined as competitive.

Finally, for α-Glu, compounds **3a–n** showed K_i values between 215 ± 29 and 625 ± 47 nM (Table 1). The results demonstrated that all compounds had effective α-Glu inhibition effects than that of acarbose (K_i: 745 ± 98 nM) as a standard α-Glu inhibitor. Also, highly effective K_i values were calculated for compound **3i** (K_i: 215 ± 29 nM). The inhibition type of the α-Glu was determined as noncompetitive. α-Glu inhibitors (AGIs) are a class of drugs that are used in the therapy of T2DM, alone or combined with other antidiabetic drugs. They may also be used in patients with impaired glucose tolerance, thus delaying the occurrence of T2DM in these patients.[41,42] They are especially beneficial for patients who are at risk of hypoglycemia or lactic acidosis, and thus are not suitable candidates for other antidiabetic drugs like metformin and sulfonylureas. The Food and Drug Administration (FDA) approves AGIs for the treatment of T2DM.[43] They have shown some benefit in T1D and gestational DM, but they are not FDA-approved for these indications. Acarbose compound has shown to reduce body weight in a worldwide observational study.[44] Recent studies on patients with

TABLE 1 The enzyme inhibition results of compounds **3a–n** against human carbonic anhydrase isoenzymes I and II (hCA I and II), acetylcholinesterase (AChE), and α-glucosidase (α-Glu) enzymes

Compound	IC_{50} (nM)								K_i (nM)			
	hCA I	r^2	hCA II	r^2	AChE	r^2	α-Glu	r^2	hCA I	hCA II	AChE	α-Glu
3a	837.32	.9591	783.22	.9441	105.38	.9372	483.26	.9384	894 ± 37	844 ± 48	88 ± 12	529 ± 45
3b	734.04	.9883	691.45	.9774	138.04	.9584	505.38	.9129	782 ± 93	735 ± 62	122 ± 10	549 ± 62
3c	912.37	.9421	849.04	.9810	111.43	.9726	591.51	.9433	988 ± 77	894 ± 91	80 ± 8	625 ± 47
3d	888.35	.9945	823.26	.9483	182.37	.9831	544.26	.9704	938 ± 54	900 ± 83	156 ± 17	589 ± 50
3e	504.57	.9889	472.35	.9904	100.04	.9625	399.84	.9952	588 ± 43	490 ± 35	81 ± 8	433 ± 27
3f	491.18	.9683	461.33	.9795	92.27	.9984	384.34	.9635	537 ± 93	498 ± 36	68 ± 7	400 ± 39
3g	201.30	.9935	172.17	.9609	81.32	.9485	415.04	.9801	244 ± 25	199 ± 25	69 ± 5	467 ± 92
3h	444.38	.9483	403.55	.9924	89.05	.9889	481.23	.9884	457 ± 48	462 ± 30	75 ± 8	513 ± 69
3i	406.94	.9669	366.78	.9624	93.47	.9424	198.37	.9768	433 ± 40	393 ± 57	80 ± 11	215 ± 29
3j	683.05	.9704	711.34	.9633	144.88	.9820	572.11	.9347	712 ± 71	743 ± 88	112 ± 15	614 ± 93
3k	495.01	.9933	458.12	.9637	104.98	.9637	429.08	.9093	529 ± 55	504 ± 43	87 ± 10	445 ± 49
3l	225.34	.9538	192.38	.9965	77.43	.9711	273.21	.9318	284 ± 28	194 ± 29	60 ± 7	278 ± 28
3m	301.24	.9126	374.04	.9505	38.94	.9408	347.04	.9394	348 ± 38	403 ± 68	30 ± 6	380 ± 80
3n	463.77	.9832	424.98	.9128	79.02	.9684	204.38	.9936	502 ± 51	458 ± 35	63 ± 6	250 ± 26
AZA	1095.47	.9782	1190.37	.9904	–	–	–	–	1137 ± 115	1210 ± 204	–	–
TAC	–	–	–	–	198.24	.9077	–	–	–	–	167 ± 24	–
ACR	–	–	–	–	–	–	711.04	.9782	–	–	–	745 ± 98

Abbreviations: ACR, acarbose; AZA, acetazolamide; TAC, tacrine.

impaired glucose resistance show that α-glycosidase inhibitors exhibit curative effects on postprandial hyperglycemia and decrease the risk of developing T2DM. Hence, it is important for the recovery and synthesis of the glucosidase inhibitors having the desired properties. Many studies have been performed to investigate the inhibitory effects of the different metal complexes on the α-Glu activity.[45]

2.3 | Molecular docking studies

The results of in vitro studies have indicated that the target compounds are potent inhibitors at the nM concentration level. In particular, compounds **3g**, **3l**, **3i**, and **3m** exhibited the best inhibitory effect on hCA I, hCA II, AChE, and α-Glu enzyme, respectively. Nevertheless, it is not yet known exactly how the most active compounds inhibited the enzyme. For these reasons, we have performed in silico studies to detect their inhibition mechanism. The first of these studies detected drug-likeness properties of compounds **3a–n**. We have analyzed their pharmaceutical properties on the basis of Lipinski's rule, toxicity, oral absorption, cell permeability, and so forth. The pharmaceutical properties are presented in Table 2. The pharmaceutical properties exactly provided Lipinski's rule of five. Also, the compounds were nontoxic and noneffective against the human ether-a-go-go-related gene (hERG) potassium channel. The results have indicated that the compounds do not have any toxic effect on human cells and are not at risk of blocking the heart hERG channel. Moreover, they exhibited excellent oral absorption and cell membrane permeability, except compound **3k**. All these properties have revealed that the compounds can exhibit good drug-likeness properties.

After detection of drug-likeness properties of the compounds, induced-fit docking studies were performed. First, the accuracy of the docking method was tested by docking the cocrystallized ligand into the active site of each enzyme. The test results were analyzed on the basis of the root-mean-square deviation (RMSD) of atomic positions. As seen in Figure 2, atomic positions cocrystallized and redocked ligands located with low RMSD values, which means that the docking method was reliable to correctly perform the prediction of the inhibition mechanism.

Then the most active compounds were docked into the catalytic active site of the enzymes and docking results were assessed on the basis of binding affinity scores and best pose of docked compounds. The highest score in the negative direction was selected as the best score, and the score is presented in Table 3. According to the scores, compounds **3g**, **3l**, and **3i** exhibited good binding affinity against hCA I, hCA II, and α-Glu enzyme, respectively. The binding affinities were quite similar to the standard inhibitor of the enzymes. However, compound **3m** exhibited better binding affinity against the AChE enzyme than its standard inhibitor. The scores have shown that the most active compounds were good inhibitors against the enzymes. Next, the best-scored pose of the most active inhibitors was selected as the best pose, which is illustrated in Figures 3 and 4, and the best pose was analyzed to understand their inhibition mechanisms.

The catalytic active site of CAs consisted of three conserved residues, His94, His96, and His119, and a water molecule. They coordinated with a zinc atom.[46] Compounds **3g** and **3l** formed close interactions with some of the residues. The 5-bromo-2-hydroxybenzylidene moiety formed π–π stacking interaction with His94 through the aromatic ring and metal coordination and salt

TABLE 2 Pharmaceutical properties of compounds **3a–n**

Compound	rtvFG	MW	DHB	AHB	logPo/w	loghERG	Caco	PMDCK (nm/s)	Hum. oral abs. (%)
3a	0	278.31	0.00	4.50	3.18	−5.97	2014	1054	100
3b	0	278.31	0.00	5.00	2.81	−5.82	1606	825.8	100
3c	0	267.28	0.00	4.00	3.12	−5.58	2869	1545	100
3d	0	283.34	0.00	3.50	3.77	−5.61	2938	2919	100
3e	0	293.32	1.00	4.25	3.27	−5.80	933.1	459.0	100
3f	0	323.35	1.00	5.00	3.39	−5.83	971.5	479.5	100
3g	0	372.22	1.00	4.25	3.88	−5.78	1123	1486	100
3h	0	327.38	0.00	3.50	4.85	−6.71	2978	1609	100
3i	0	343.38	1.00	4.25	4.28	−6.06	1849	961.6	100
3j	0	337.37	0.00	5.00	4.15	−5.76	3839	2117	100
3k	2	324.33	2.00	4.50	3.01	−5.90	298.8	134.1	89
3l	0	346.21	0.00	3.50	4.77	−5.77	2995	8079	100
3m	0	345.32	0.00	3.50	4.75	−5.69	3233	6299	100
3n	0	444.53	0.00	4.00	7.15	−8.28	3031	1640	100

Abbreviations: AHB, number of hydrogen bond acceptors; Caco, Caco-2 cell membrane permeability; DHB, number of hydrogen bond donors; Hum. oral abs., qualitative human oral absorption; loghERG, IC_{50} value for blockage of hERG K^+ channels; logPo/w, octanol/water partition coefficient; MW, molecular weight; PMDCK, MDCK cell permeability; rtvFG, reactive group (tox).

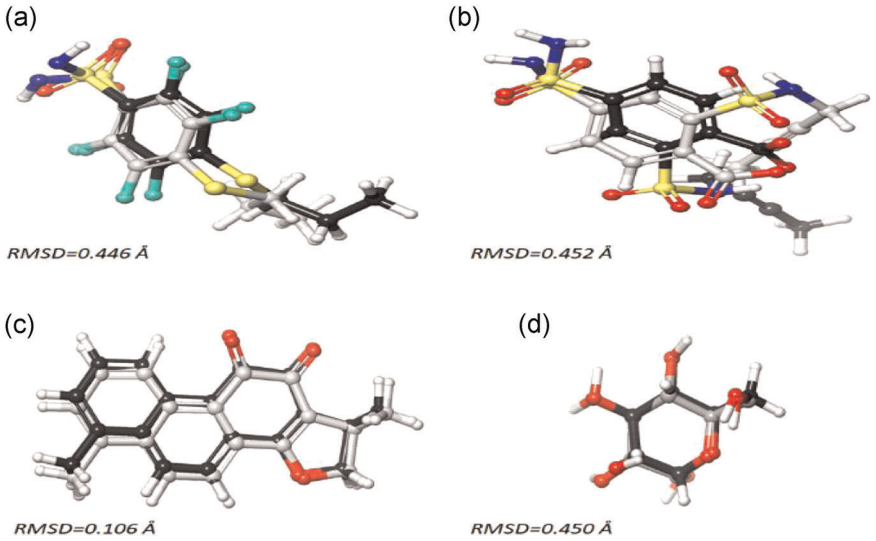

FIGURE 2 Induced-fit docking method validation. (a) 3TV-hCA I, (b) 51j-hCA II, (c) 1YL-AChE, and (d) D-glucose-α-glucosidase. Cocrystallized ligands were represented with the black ball-and-stick model and redocked ligands were represented with a gray ball-and-stick model.
AChE, acetylcholinesterase; hCA, human carbonic anhydrase; RMSD, root-mean-square deviation

bridge with the zinc atom (Figure 3a). The interactions between the deprotonated hydroxyl group and zinc atom were quite similar to those of inhibitors containing a sulfonamide group.[47] In addition to these interactions, quinazoline moiety formed two π–π stacking interactions with His200. Compound **3l** most actively inhibited hCA II enzyme, and its quinazolinone moiety was majorly responsible for the enzyme inhibition. As the quinazolinone moiety was located in the catalytic active site, 2,4-dichlorobenzylidene moiety stayed out of the site, as seen in Figure 4b. The quinazolinone moiety formed π–π stacking interactions with His94. Although it could not form coordination with the zinc atom, the oxygen atom of the moiety formed a hydrogen bond by receiving hydrogen from Asn67 and Gln92 (Figure 3b). Because Gln92 formed a hydrogen bond with His94, the indirect interaction of Gln92 with the zinc atom contributes toward the catalytic activity of the enzyme.[48] Therefore, the interactions have contributed to enzyme inhibition by forming an effective network between active site components.

TABLE 3 Binding affinities (kcal/mol) of the most active compounds against hCA I, hCA II, AChE, and α-glucosidase enzymes

Compounds	Glide score (kcal/mol)			
	hCA I	hCA II	AChE	α-Glu
3g	−7.636	–	–	–
3l	–	−6.972	–	–
3m	–	–	−10.080	–
3i	–	–	–	−8.486
AZA[a]	−9.016	−9.560	–	–
TAC[b]	–	–	−9.579	–
ACR[c]	–	–	–	−16.933

Abbreviations: AChE, acetylcholinesterase; hCA, human carbonic anhydrase; α-Glu, α-glucosidase.

[a]Acetazolamide (AZA) was used as a standard inhibitor for human carbonic anhydrase isoenzymes I and II (hCA I and II).

[b]Tacrine (TAC) was used as a standard inhibitor for the acetylcholinesterase (AChE) enzyme.

[c]Acarbose (ACR) was used as a standard inhibitor for the α-glycosidase enzyme.

Compound **3m** is the most active compound in **3a-n** and highly effective against AChE enzyme, even its standard inhibitor. The effectiveness was derived from hydrophobic interactions between aromatic rings and active site residues. As seen in Figure 3c, 2-trifluoromethylbenzylidene and quinazolinone moieties formed many π–π stacking interactions with Tyr72, Trp286, Tyr341, and Tyr337. The nitrogen atom of quinazolinone moiety interacted with Asp74 via a water bridge (Figure 4c). Also, the modes of binding of **3m** within the peripheral site have indicated that it is very well located in a catalytic active site gorge. Ashani et al.[49] have revealed that Tyr337 residue plays a vital role in enzyme activity. Many potent AChE inhibitors inhibit the enzyme activity by interacting with similar catalytic active site residues.[50–52] The catalytic active site of the α-Glu enzyme is constituted of many charged residues,[53] which enables the compound to form hydrogen bonds. The oxygen atom of quinazolinone and 2-hydroxynaphthalene moieties interacted with Gln279 and Gln353. Besides, the quinazolinone and 2-hydroxynaphthalen moieties formed π–π stacking interactions with Phe178 and Phe303 via aromatic rings. Also, 2-hydroxynaphthalen formed π–cation interactions with Arg315, as seen in Figure 3d. In addition, the compound formed aromatic hydrogen bonds with Thr306 and Asp307 (Figure 4d). The enzyme has gatekeeper residues at the entrance of its active site[54] and Phe303 is one of the gatekeeper residues. The interaction between the residue and **3i** may cause enzyme inhibition by blocking the catalytic active site entrance.

3 | CONCLUSION

In this study, novel quinazolinone derivatives were synthesized from different aldehydes and 2-ethyl-3-aminoquinazolin-4(3*H*)-one. Structures of the novel compounds were characterized by ^{1}H and ^{13}C NMR, IR spectroscopy, and HRMS. Novel compounds were

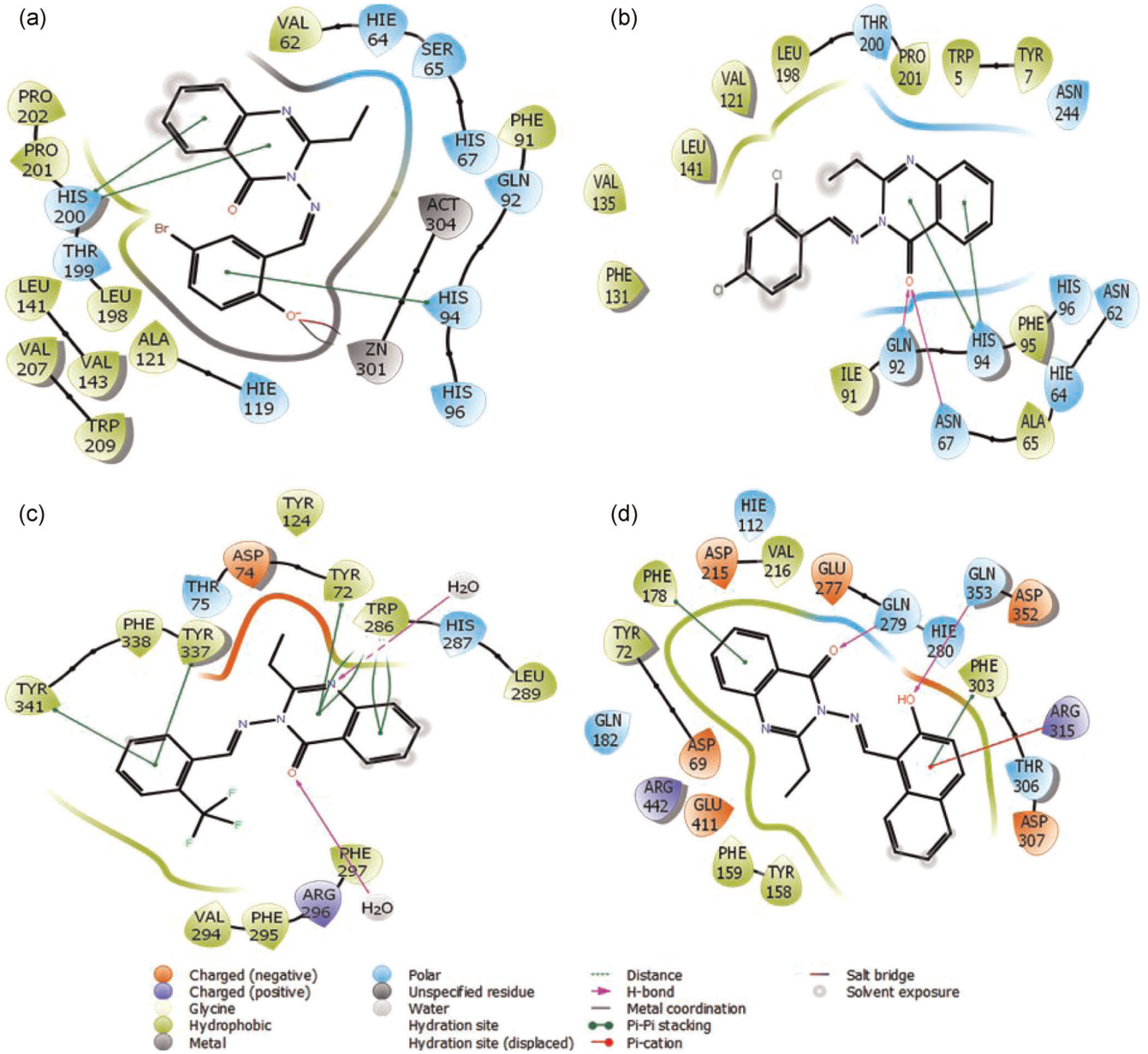

FIGURE 3 2D interaction modes of best-posed novel quinazolinon derivatives into catalytic active sites of the enzymes. (a) **3g**-hCA I, (b) **3l**-hCA II, (c) **3m**-AChE, and (d) **3i**-α-glucosidase. 2D, two-dimensional; AChE, acetylcholinesterase; hCA, human carbonic anhydrase

tested against some metabolic enzymes including α-Glu, AChE, hCA I, and hCA II enzymes. According to the results of enzyme inhibition studies, compounds **3g**, **3i**, **3l**, and **3m** are good potential inhibitors for these enzymes.

We have also revealed the predicted inhibition mechanism of the most active compounds against the enzymes. According to the molecular docking results, their aromatic rings played a critical role in forming hydrophobic interaction with active site residues of each enzyme. Also, oxygen providing polar interactions has received attention due to the contribution to α-Glu inhibition.

Finally, according to the results of in vitro and in silico studies, we hope that our findings lead to the design of new inhibitors against the enzymes. Also, we hope that our novel molecules are good candidate drugs after advanced research.

4 | EXPERIMENTAL

4.1 | Chemistry

4.1.1 | General

The chemicals used in this study were supplied from Sigma Aldrich (Germany). Melting points (mp) were determined on a WRS-2A

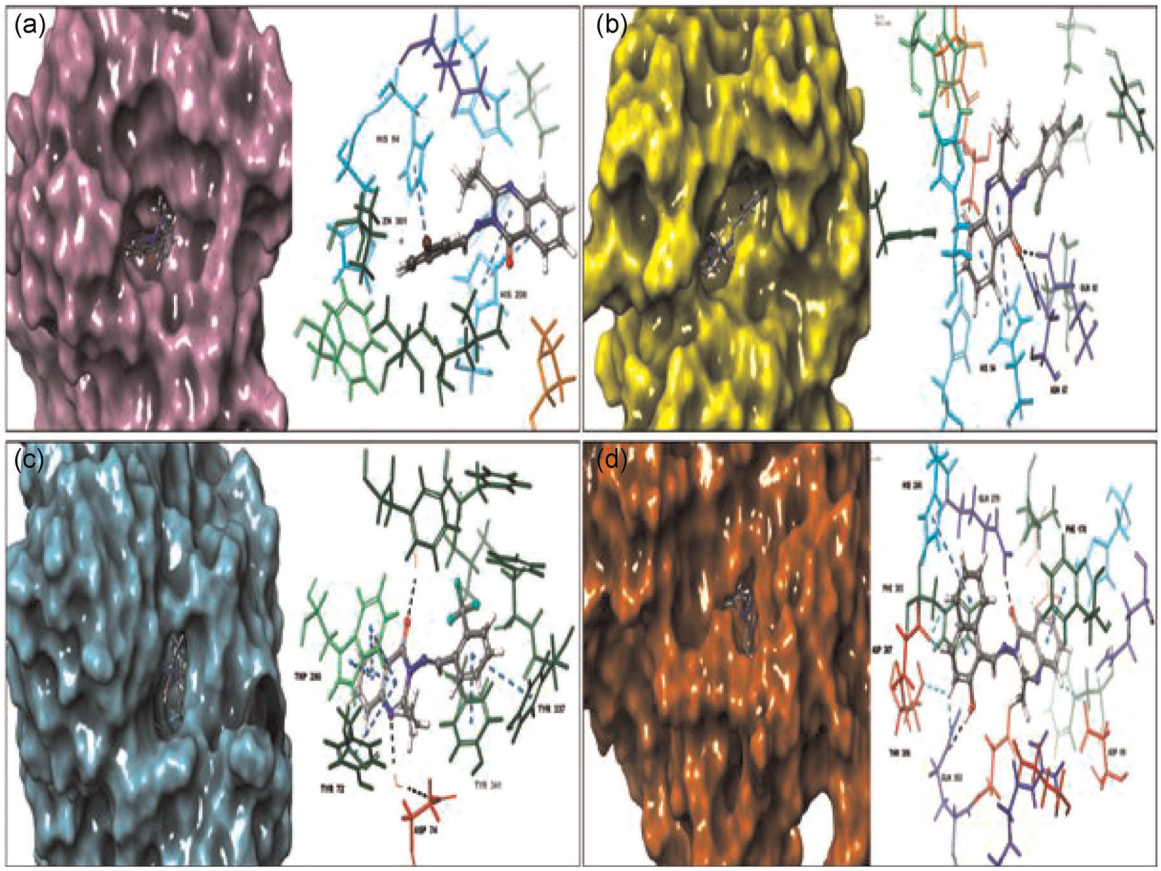

FIGURE 4 Superimposition of best-posed novel quinazolinon derivatives into catalytic active sites of the enzymes. (a) **3g**-hCA I, (b) **3l**-hCA II, (c) **3m**-AChE, and (d) **3i**-α-glucosidase. Most active novel quinazolinone derivatives have been represented with the gray ball-and-stick model. The enzymes have been represented with colored ribbons. Hydrogen bonds have been represented with a black dashed line. π–π stacking interactions have been represented with a blue dashed line. Aromatic hydrogen bonds have been represented with a turquoise dashed line. AChE, acetylcholinesterase; hCA, human carbonic anhydrase

microprocessor melting-point apparatus and were uncorrected. IR spectra of compounds were recorded using an Alpha-P Bruker FT-IR spectrophotometer. ^{1}H-NMR spectra (see the Supporting Information) were recorded on a Bruker (400 MHz) spectrometer. ^{13}C-NMR spectra were recorded on a Bruker (100 MHz) spectrometer. Chemical shifts are reported as δ in ppm, relative to tetramethylsilane (δ 0.00 singlet) in deuterated dimethylsulfoxide (DMSO-d_6) (for compounds **3** and **3e**) and deuterated chloroform ($CDCl_3$). HRMS spectra were recorded on an Agilent 6530 Accurate mass spectrometer and acetonitrile was used as the solvent.

The InChI codes of the investigated compounds, together with some biological activity data, are provided as Supporting Information.

4.1.2 | Synthesis of methyl 2-propionamidobenzoate (**2**)

To a solution of methyl anthranilate (**1**) (10 mmol) in tetrahydrofuran (20 ml), triethylamine (11 mmol) and propionyl chloride (10 mmol) were added dropwise, respectively, at 0–5°C, and the mixture was stirred at this temperature for half an hour. Then, the mixture was refluxed for 3 h. The reaction progress was monitored by thin-layer chromatography (TLC) (hexane/ethyl acetate 9:1). After completion, the solvent was removed under reduced pressure and cold water (100 ml) was added. The mixture was stirred well and the crude product was filtered and used in the next step without any purification. Colorless solid, mp: 34–35°C (lit: 33°C).[55]

4.1.3 | Synthesis of 3-amino-2-ethylquinazolin-4(3*H*)-one (**3**)

To a solution of methyl 2-propionamidobenzoate (**2**) (10 mmol) in ethanol (20 ml), hydrazinium hydroxide (25 mmol) was added, and the mixture was refluxed for 4 h. Reaction progress was monitored by TLC (hexane/ethyl acetate 9:1) (Scheme 1). After completion, 50% of the solvent was removed under reduced pressure and diethyl ether (20 ml) was added. The mixture was left in the freezer overnight and the formed white crystals were filtered off. The crude product was recrystallized from ethanol/diethyl ether (1:2). Yield: 87%, mp: 124–125°C (lit: 122–123°C).[56] ^{1}H-NMR (400 MHz, DMSO-d_6, δ/ppm): δ 8.12 (d, J = 7.6 Hz, 1H), 7.79 (t, J = 7.5 Hz, 1H), 7.64 (d, J = 8.0 Hz, 1H), 7.48

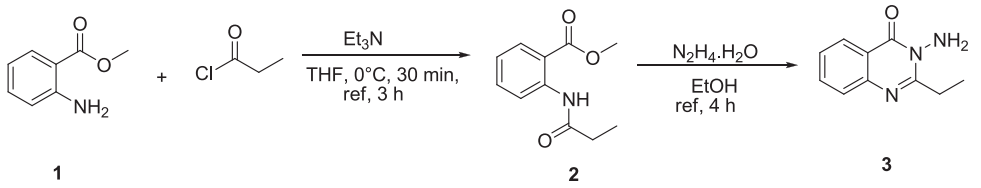

SCHEME 1 Synthesis of 3-amino-2-ethylquinazolin-4(*3H*)-one (**3**)

(t, *J* = 7.5 Hz, 1H), 5.75 (s, 2H), 2.98 (q, *J* = 7.4 Hz, 2H), and 1.29 (t, *J* = 7.4 Hz, 3H); ^{13}C-NMR (100 MHz, DMSO-d_6, *δ*/ppm): *δ* 160.4, 159.0, 146.6, 133.9, 126.8, 125.9, 125.8, 119.8, 26.9, and 10.6.

4.1.4 | General procedure for the synthesis of compounds **3a–n**

To a solution of 3-amino-2-ethylquinazolin-4(*3H*)-one (**3**) (10 mmol) in glacial acetic acid (10 ml), substituted benzaldehyde (10 mmol) was added, and the mixture was refluxed for an hour (Scheme 2). Reaction progress was monitored by TLC (hexane/ethyl acetate 7:3). The solvent was evaporated and the crude product was recrystallized from ethanol. The structures of compounds **3a–n** are given in Figure 1.

*2-Ethyl-3-[(pyridin-2-ylmethylene)amino]quinazolin-4(3H)-one (**3a**)*
Beige solid, yield: 90%, mp: 143–145°C, IR (ATR, cm^{-1}) ν_{max}: 3083, 3011, 2984, 1678, 1602, 1466, 1214, 767, and 685; ^{1}H-NMR (400 MHz, $CDCl_3$, *δ*/ppm): *δ* 9.21 (s, 1H), 8.76 (d, *J* = 4.7 Hz, 1H), 8.31 (dd, *J* = 8.0, 1.3 Hz, 1H), 8.19 (d, *J* = 7.8 Hz, 1H), 7.85 (t, *J* = 7.7 Hz, 1H), 7.79–7.68 (m, 2H), 7.49–7.42 (m, 2H), 3.02 (q, *J* = 7.4 Hz, 2H), and 1.38 (t, *J* = 7.4 Hz, 3H); ^{13}C-NMR (101 MHz, $CDCl_3$, *δ*/ppm): *δ* 166.3, 158.6, 157.5, 152.3, 150.1, 146.5, 136.7, 134.4, 127.4, 127.2, 126.5, 125.8, 121.9, 121.5, 28.6, and 11.1; HRMS (Q-TOF) *m/z* calcd for $C_{16}H_{14}N_4O$ [M+H]$^+$: 279.1246, Found: 279.1243.

*2-Ethyl-3-[(pyridin-4-ylmethylene)amino]quinazolin-4(3H)-one (**3b**)*
Beige solid, yield: 92%, mp:139–141°C, IR (ATR, cm^{-1}) ν_{max}: 3037, 2983, 2940, 1678, 1593, 1466, 1215, 763, and 664; ^{1}H-NMR (400 MHz, $CDCl_3$, *δ*/ppm): *δ* 9.38 (s, 1H), 8.80 (d, *J* = 5.9 Hz, 2H), 8.29 (d, *J* = 8.0 Hz, 1H), 7.79–7.70 (m, 4H), 7.49 (t, *J* = 7.5 Hz, 1H), 3.05 (q, *J* = 7.4 Hz, 2H), and 1.40 (t, *J* = 7.4 Hz, 3H); ^{13}C-NMR (101 MHz, $CDCl_3$, *δ*/ppm): *δ* 161.8, 159.3, 157.7, 150.8, 146.3, 140.5, 134.6, 127.3, 126.7, 122.0, 121.4, 28.7, and 11.2; HRMS (quadrupole time-of-flight [Q-TOF]) *m/z* calcd for $C_{16}H_{14}N_4O$ [M+H]$^+$: 279.1246, Found: 279.1247.

*2-Ethyl-3-[(furan-2-ylmethylene)amino]quinazolin-4(3H)-one (**3c**)*
White solid, yield: 89%, mp: 149–151°C, IR (ATR, cm^{-1}) ν_{max}: 3129, 3068, 3012, 2975, 1671, 1594, 1469, 1282, 761, and 685; ^{1}H-NMR (400 MHz, $CDCl_3$, *δ*/ppm): *δ* 8.89 (s, 1H), 8.28 (d, *J* = 8.0 Hz, 1H), 7.76–7.69 (m, 3H), 7.46 (t, *J* = 8.1 Hz, 1H), 7.06 (d, *J* = 4.0 Hz, 1H),

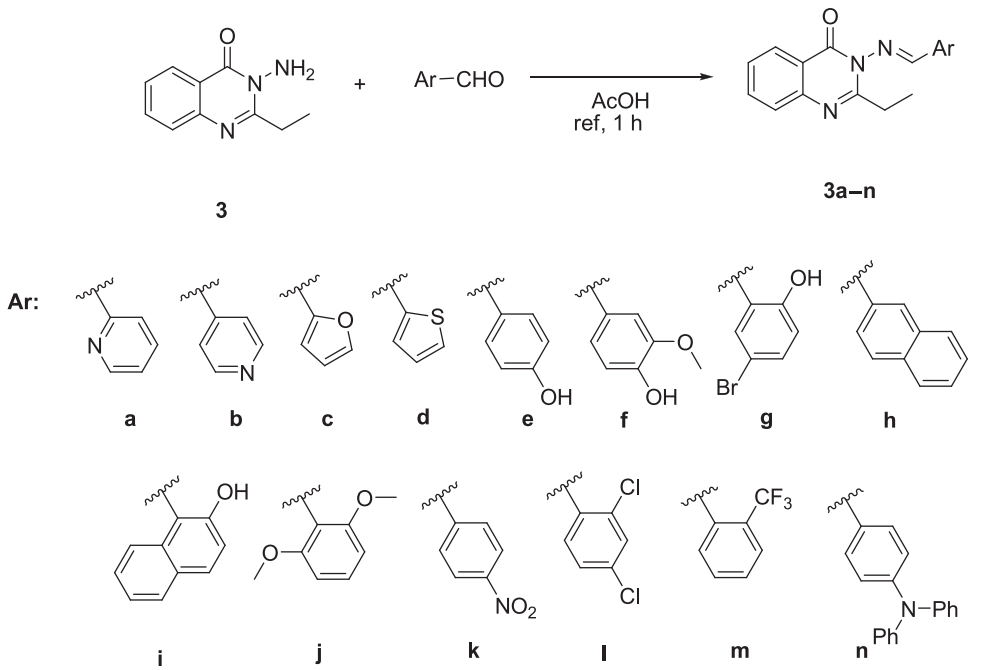

SCHEME 2 Synthesis of compounds **3a–n**

6.61 (dd, J = 3.5, 1.7 Hz, 1H), 3.01 (q, J = 7.4 Hz, 2H), and 1.37 (t, J = 7.4 Hz, 3H); ^{13}C-NMR (101 MHz, $CDCl_3$, δ/ppm): δ 158.9, 157.6, 154.5, 148.3, 146.8, 146.5, 134.3, 127.2, 126.4, 121.3, 118.4, 112.5, 28.5, and 11.1; HRMS (Q-TOF) m/z calcd for $C_{15}H_{13}N_3O_2$ $[M+H]^+$: 268.1086, Found: 268.1088.

*2-Ethyl-3-[(thiophene-2-ylmethylene)amino]quinazolin-4(3H)-one (**3d**)*

White solid, yield: 88%, mp: 122–124°C, IR (ATR, cm^{-1}) ν_{max}: 3099, 2979, 2936, 1662, 1591, 1466, 1284, 764, and 710; ^{1}H-NMR (400 MHz, $CDCl_3$, δ/ppm): δ 9.26 (s, 1H), 8.28 (d, J = 7.9 Hz, 1H), 7.76–7.68 (m, 2H), 7.59 (d, J = 4.9 Hz, 1H), 7.54 (d, J = 3.4 Hz, 1H), 7.45 (t, J = 7.3 Hz, 1H), 7.19–7.15 (m, 1H), 2.99 (q, J = 7.4 Hz, 2H), and 1.37 (t, J = 7.4 Hz, 3H); ^{13}C-NMR (101 MHz, $CDCl_3$, δ/ppm): δ 159.4, 157.7, 146.5, 137.8, 134.2, 134.1, 131.5, 128.0, 127.2, 126.4, 121.4, 28.6, and 11.1; HRMS (Q-TOF) m/z calcd for $C_{15}H_{13}N_3OS$ $[M+H]^+$: 284.0858, Found: 284.0858.

*2-Ethyl-3-[(4-hydroxybenzylidene)amino]quinazolin-4(3H)-one (**3e**)*

White solid, yield: 93%, mp: 264–265°C, IR (ATR, cm^{-1}) ν_{max}: 3167, 3018, 2981, 2938, 1632, 1578, 1469, 1272, 836, 717, and 691; ^{1}H-NMR (400 MHz, DMSO-d_6, δ/ppm): δ 10.39 (s, 1H), 8.74 (s, 1H), 8.14 (d, J = 7.9 Hz, 1H), 7.81 (d, J = 7.8 Hz, 3H), 7.68 (d, J = 8.2 Hz, 1H), 7.51 (t, J = 7.5 Hz, 1H), 6.95 (d, J = 8.3 Hz, 2H), 2.83 (q, J = 7.3 Hz, 2H), and 1.25 (t, J = 7.3 Hz, 3H); ^{13}C-NMR (101 MHz, DMSO-d_6, δ/ppm): δ 169.4, 161.8, 157.5, 156.7, 146.3, 134.1, 130.9, 126.9, 126.5, 126.2, 123.3, 120.9, 116.0, 27.4, and 10.4; HRMS (Q-TOF) m/z calcd for $C_{17}H_{15}N_3O_2$ $[M+H]^+$: 294.1243, Found: 294.1237.

*2-Ethyl-3-[(4-hydroxy-3-methoxybenzylidene)amino]quinazolin-4(3H)-one (**3f**)*

White solid, yield: 85%, mp: 162–164°C, IR (ATR, cm^{-1}) ν_{max}: 3056, 2975, 2935, 1669, 1569, 1468, 1283, 825, 720, and 689; ^{1}H-NMR (400 MHz, $CDCl_3$, δ/ppm): δ 8.75 (s, 1H), 8.29 (d, J = 8.5 Hz, 1H), 7.78–7.68 (m, 2H), 7.56 (s, 1H), 7.46 (t, J = 8.1 Hz, 1H), 7.30 (dd, J = 8.1, 1.8 Hz, 1H), 7.01 (d, J = 8.1 Hz, 1H), 3.97 (s, 3H), 2.98 (q, J = 7.4 Hz, 2H), and 1.37 (t, J = 7.4 Hz, 3H); ^{13}C-NMR (101 MHz, $CDCl_3$, δ/ppm): δ 167.5, 158.8, 157.5, 150.2, 147.2, 146.6, 134.2, 127.2, 127.1, 126.3, 125.4, 125.0, 121.4, 114.7, 108.9, 56.1, 28.5, and 11.1; HRMS (Q-TOF) m/z calcd for $C_{18}H_{17}N_3O_3$ $[M+H]^+$: 324.1348, Found: 324.1344.

*2-Ethyl-3-[(5-bromo-2-hydroxybenzylidene)amino]quinazolin-4(3H)-one (**3g**)*

White solid, yield: 92%, mp: 193–195°C, IR (ATR, cm^{-1}) ν_{max}: 3068, 3038, 2981, 2934, 1675, 1600, 1468, 1272, 736, and 688; ^{1}H-NMR (400 MHz, $CDCl_3$, δ/ppm): δ 10.82 (s, 1H), 8.99 (s, 1H), 8.31 (dd, J = 8.0, 1.2 Hz, 1H), 7.80–7.76 (m, 2H) 7.59–7.47 (m, 3H), 7.01 (d, J = 8.8 Hz, 1H), 2.96 (q, J = 7.4 Hz, 2H), and 1.41 (t, J = 7.4 Hz, 3H); ^{13}C-NMR (101 MHz, $CDCl_3$, δ/ppm): δ 169.5, 159.1, 158.4, 155.9, 146.1, 137.1, 135.3, 134.8, 127.4, 127.3, 126.9, 121.0, 119.5, 117.9, 111.5, 28.4, and 10.9; HRMS (Q-TOF) m/z calcd for $C_{17}H_{14}BrN_3O_2$ $[M+H]^+$: 372.0348, Found: 372.0345.

*2-Ethyl-3-[(naphthalen-2-ylmethylene)amino]quinazolin-4(3H)-one (**3h**)*

White solid, yield: 90%, mp: 156–157°C, IR (ATR, cm^{-1}) ν_{max}: 3059, 3030, 2970, 2943, 1671, 1589, 1465, 1278, 752, and 692; ^{1}H-NMR (400 MHz, $CDCl_3$, δ/ppm): δ 9.22 (s, 1H), 8.34 (d, J = 8.5 Hz, 1H), 8.19 (dd, J = 10.8, 2.2 Hz, 2H), 7.98–7.92 (m, 3H), 7.82–7.70 (m, 2H), 7.67–7.55 (m, 2H), 7.50 (t, J = 8.1 Hz, 1H), 3.08 (q, J = 7.4 Hz, 2H), and 1.43 (t, J = 7.4 Hz, 3H); ^{13}C-NMR (101 MHz, $CDCl_3$, δ/ppm): δ 166.6, 158.9, 135.4, 134.3, 133.0, 132.4, 130.5, 129.0, 128.2, 128.0, 127.3, 127.1, 126.4, 122.9, 121.5, 28.6, and 11.2; HRMS (Q-TOF) m/z calcd for $C_{21}H_{17}N_3O$ $[M+H]^+$: 328.1450, Found: 328.1447.

*2-Ethyl-3-{[(2-hydroxynaphthalen-1-yl)methylene]amino}quinazolin-4(3H)-one (**3i**)*

White solid, yield: 91%, mp: 187–188°C, IR (ATR, cm^{-1}) ν_{max}: 3059, 2985, 2939, 1671, 1596, 1466, 1280, 757, and 683; ^{1}H-NMR (400 MHz, $CDCl_3$, δ/ppm): δ 12.30 (s, 1H), 9.89 (s, 1H), 8.35 (d, J = 8.4 Hz, 1H), 8.05 (d, J = 8.5 Hz, 1H), 7.97 (d, J = 9.0 Hz, 1H), 7.85–7.79 (m, 3H), 7.60–7.51 (m, 2H), 7.44 (t, J = 7.5 Hz, 1H), 7.30–7.27 (m, 1H), 3.02 (q, J = 7.4 Hz, 2H), and 1.44 (t, J = 7.4 Hz, 3H); ^{13}C-NMR (101 MHz, $CDCl_3$, δ/ppm): δ 167.9, 161.7, 158.7, 156.3, 136.3, 134.6, 132.9, 129.3, 128.5, 128.2, 127.3, 127.2, 126.8, 124.2, 121.2, 120.0, 119.2, 107.3, 28.5, and 11.0; HRMS (Q-TOF) m/z calcd for $C_{21}H_{17}N_3O_2$ $[M+H]^+$: 344.1399, Found: 344.1398.

*2-Ethyl-3-[(2,6-dimethoxybenzylidene)amino]quinazolin-4(3H)-one (**3j**)*

White solid, yield: 89%, mp: 171–173°C, IR (ATR, cm^{-1}) ν_{max}: 3049, 3019, 2990, 2929, 1680, 1606, 1582, 1469, 1260, 772, and 688; ^{1}H-NMR (400 MHz, $CDCl_3$, δ/ppm): δ 9.29 (s, 1H), 8.32 (d, J = 7.5 Hz, 1H), 7.78–7.70 (m, 3H), 7.47 (t, J = 8.1 Hz, 1H), 7.11 (dd, J = 9.1, 3.2 Hz, 1H), 6.94 (d, J = 9.1 Hz, 1H), 3.87 (s, 6H), 2.99 (q, J = 7.4 Hz, 2H), and 1.39 (t, J = 7.4 Hz, 3H); ^{13}C-NMR (101 MHz, $CDCl_3$, δ/ppm): δ 163.9, 158.6, 157.6, 154.4, 153.6, 134.1, 127.3, 127.0, 126.3, 121.4, 120.9, 112.8, 110.4, 56.2, 55.9, 28.4, and 11.1; HRMS (Q-TOF) m/z calcd for $C_{19}H_{19}N_3O_3$ $[M+H]^+$: 338.1505, Found: 338.1499.

*2-Ethyl-3-[(4-nitrobenzylidene)amino]quinazolin-4(3H)-one (**3k**)*

White solid, yield: 93%, mp:195–197°C,[57] IR (ATR, cm^{-1}) ν_{max}: 3112, 3043, 2981, 2923, 1670, 1607, 1517, 1335, 1243, 833, and 692; ^{1}H-NMR (400 MHz, $CDCl_3$, δ/ppm): δ 9.47 (s, 1H), 8.37 (d, J = 8.6 Hz, 2H), 8.31 (d, J = 8.0 Hz, 1H), 8.08 (d, J = 8.6 Hz, 2H), 7.83–7.70 (m, 2H), 7.51 (t, J = 7.4 Hz, 1H), 3.07 (q, J = 7.4 Hz, 2H), and 1.42 (t, J = 7.4 Hz, 3H); ^{13}C-NMR (101 MHz, $CDCl_3$, δ/ppm): δ 161.6, 159.2, 157.7, 149.8, 146.1, 139.0, 134.7, 129.3, 127.3, 127.3, 126.8, 124.2, 121.4, 28.7, and 11.2; HRMS (Q-TOF) m/z calcd for $C_{17}H_{14}N_4O_3$ $[M+H]^+$: 323.1144, Found: 323.1141.

*2-Ethyl-3-[(4-nitrobenzylidene)amino]quinazolin-4(3H)-one (**3l**)*

White solid, yield: 90%, mp: 173–174°C, IR (ATR, cm^{-1}) ν_{max}: 3048, 3018, 2969, 2929, 1680, 1606, 1582, 1469, 1293, 772, and 689; ^{1}H-NMR (400 MHz, $CDCl_3$, δ/ppm): δ 9.58 (s, 1H), 8.32 (d, J = 9.2 Hz, 1H), 8.18 (d, J = 8.5 Hz, 1H), 7.82–7.68 (m, 2H), 7.55–7.44 (m, 2H),

7.41 (d, J = 8.5 Hz, 1H), 3.02 (q, J = 7.4 Hz, 2H), and 1.40 (t, J = 7.4 Hz, 3H); ^{13}C-NMR (101 MHz, $CDCl_3$, δ/ppm): δ 161.5, 158.8, 157.6, 138.8, 136.9, 134.5, 130.1, 129.4, 128.8, 127.9, 127.4, 127.1, 126.6, 121.4, 28.6, and 11.1; HRMS (Q-TOF) m/z calcd for $C_{17}H_{13}Cl_2N_3O$ $[M+H]^+$: 346.0514, Found: 346.0511.

*2-Ethyl-3-[(2-trifluoromethylbenzylidene)amino]quinazolin-4(3H)-one (**3m**)*

White solid, yield: 87%, mp: 128–129°C, IR (ATR, cm^{-1}) ν_{max}: 3064, 2992, 2946, 1683, 1602, 1473, 1278, 1120, 769, and 692; ^{1}H-NMR (400 MHz, $CDCl_3$, δ/ppm): δ 9.56 (s, 1H), 8.41 (d, J = 7.7 Hz, 1H), 8.34 (d, J = 7.5 Hz, 1H), 7.84–7.64 (m, 5H), 7.50 (t, J = 8.1 Hz, 1H), 3.04 (q, J = 7.4 Hz, 2H), and 1.40 (t, J = 7.4 Hz, 3H); ^{13}C-NMR (101 MHz, $CDCl_3$, δ/ppm): δ 162.7, 158.7, 157.8, 146.0, 143.7, 134.6, 132.3, 131.8, 131.0, 130.3, 130.0, 128.1, 127.5, 126.9, 126.7, 126.1, 121.3, 28.5, and 11.2; HRMS (Q-TOF) m/z calcd for $C_{18}H_{14}F_3N_3O$ $[M+H]^+$: 346.1167, Found: 346.1159.

*2-Ethyl-3-[(4-(diphenylamino)benzylidene)amino]quinazolin-4(3H)-one (**3n**)*

Yellow solid, yield: 88%, mp: 171–173°C, IR (ATR, cm^{-1}) ν_{max}: 3060, 2972, 2925, 1699, 1585, 1486, 1277, 756, and 695; ^{1}H-NMR (400 MHz, $CDCl_3$, δ/ppm): δ 8.79 (s, 1H), 8.31 (d, J = 8.0 Hz, 1H), 7.75 (dd, J = 6.5, 4.8 Hz, 4H), 7.52–7.44 (m, 1H), 7.39–7.31 (m, 4H), 7.24–7.13 (m, 6H), 7.09 (d, J = 8.7 Hz, 2H), 3.02 (q, J = 7.4 Hz, 2H), and 1.39 (t, J = 7.4 Hz, 3H); ^{13}C-NMR (101 MHz, $CDCl_3$, δ/ppm): δ 152.0, 146.5, 134.3, 130.3, 129.7, 127.3, 125.9, 124.6, 120.6, 28.2, and 11.2; HRMS (Q-TOF) m/z calcd for $C_{29}H_{24}N_4O$ $[M+H]^+$: 445.2028, Found: 445.2038.

4.2 | Bioactivity studies

In the present study, hCA I and II isoenzymes were purified by Sepharose-4B-L-tyrosine-sulfanilamide affinity column chromatography, and CA isoenzymes' activity was determined according to the spectrophotometric method of Verpoorte et al.,[58] as described in our previous studies[59,60] in detail. p-Nitrophenylacetate (p-NPA) was used as a substrate for the enzymatic reaction. One CA enzyme unit is adopted as the amount of CA, with absorbance difference at 348 nm for 3 min at 25°C. For determination of inhibition kinetics of compounds **3a–n**, an activity (%) graph was drawn. From these graphs, half-maximal inhibitor concentrations (IC_{50}) for novel compounds were determined.[61] Also, for K_i values, three different concentrations of novel compounds were used. Then, Lineweaver–Burk graphs were drawn according to these measurements. K_i values of novel compounds were determined from Lineweaver–Burk graphs, as previously described.[62] To determine the quantity of protein during the purification process, Bradford's[63] technique was utilized, where bovine serum albumin was used as the standard protein.[64] The inhibitory effect of compounds **3a–n** on AChE activity was analyzed according to the spectrophotometric method of Ellman,[65] as described previously.[66,67] The α-Glu inhibition effect of novel compounds was evaluated according to the method of Tao et al.[68] The absorbance of samples was recorded at 405 nm.[69]

4.3 | Molecular docking studies

Crystal structures of hCA I (PDB ID: 4WR7), hCA II (PDB ID: 5AML), AChE (PDB ID: 4M0E), and α-Glu (PDB ID: 3A4A) enzymes were downloaded from the RCSB website (http://www.rcsb.org/). The structures were chosen due to their high resolution and cocrystallized ligand. All compounds were prepared with the Ligprep module[70] according to the method described in previous studies.[71] Then, the pharmacokinetic properties of the compounds were calculated using the Qikprop module.[72] The structures were made ready for docking studies using the Protein Preparation Wizard module.[73] The protein preparation was performed according to the method described in previous studies.[74] Binding sites of enzymes were predicted using the Sitemap module[75] for the detection of binding sites. Binding site prediction and evaluation of the sites were performed according to the method described in previous studies.[71] The induced-fit docking method[76] was tested with the redocking process before the compounds were docked and after molecular docking studies of the most effective compounds were performed using the induced-fit docking module.[71]

CONFLICTS OF INTEREST

The authors declare that there are no conflicts of interest.

ORCID

Parham Taslimi http://orcid.org/0000-0002-3171-0633

Muhammet Karaman http://orcid.org/0000-0002-0155-3390

REFERENCES

[1] H. J. Park, Y. S. Kim, J. S. Kim, E. J. Lee, Y. J. Yi, H. J. Hwang, M. E. Suh, C. K. Ryu, S. K. Lee, *Bioorg. Med. Chem. Lett.* **2004**, *14*, 3385. https://doi.org/10.1016/j.bmcl.2004.04.094

[2] Z. Ma, Y. Hano, T. Nomura, Y. Chen, *Bioorg. Med. Chem. Lett.* **2004**, *14*, 1193. https://doi.org/10.1016/j.bmcl.2003.12.048

[3] N. Malecki, P. Carato, B. Riao, J. F. Goosens, R. Houssin, C. Bailly, J. P. Henichart, *Bioorg. Med. Chem.* **2004**, *12*, 641. https://doi.org/10.1016/j.bmc.2003.10.014

[4] V. M. Sharma, P. Prasana, K. V. Adiseshu, C. L. L. Rao, G. S. Kumar, C. P. Narasimhulu, P. A. Babu, R. C. Puranik, D. Subramanyam, A. V. Warlu, S. Rajagopal, K. B. S. Kumar, R. Ajaykumar, R. Rajagopalan, *Bioorg. Med. Chem. Lett.* **2002**, *12*, 2303. https://doi.org/10.1016/S0960-894X(02)00431-6

[5] R. J. Abdel-Jalil, H. M. Aldoqum, M. T. Ayoub, W. Voelter, *Heterocycles* **2005**, *65*, 2061. https://doi.org/10.1002/chin.200602167

[6] A. S. El-Azab, K. E. H. ElTahir, *Bioorg. Med. Chem. Lett.* **2012**, *22*, 1879. https://doi.org/10.1016/j.bmcl.2012.01.071

[7] J. Chevalier, A. Mahamoud, M. Baitiche, E. Adam, M. Viveiros, A. Smarandache, A. Militaru, M. L. Pascu, L. Amaral, J. M. Pagés, *Int. J. Antimicrob. Agents* **2010**, *36*, 163. https://doi.org/10.1016/j.ijantimicag.2010.03.027

[8] A. Mahamoud, J. Chevalier, M. Baitiche, E. Adam, J. M. Pagés, *Microbiology* **2011**, *57*, 566. https://doi.org/10.1099/mic.0.045716-0

[9] A. Gangjee, O. O. Adair, M. Pagley, S. F. Queener, *J. Med. Chem.* **2008**, *19*, 6195. https://doi.org/10.1021/jm800694g

[10] E. Manivannan, S. C. Chaturvedi, *Bioorg. Med. Chem.* **2011**, *19*, 4520. https://doi.org/10.1016/j.bmc.2011.06.019

[11] M. K. Shivananda, B. S. Holla, *J. Chem. Pharm. Res.* **2011**, *3*, 83.
[12] K. Bajaj, V. K. Srivastava, A. Kumar, *Arzneim. Forsch.* **2003**, *53*, 480. https://doi.org/10.1055/s-0031-1297137
[13] M. Amir, I. Ali, M. Z. Hassan, *Arch. Pharm. Res.* **2013**, *36*, 61. https://doi.org/10.1007/s12272-013-0004-y
[14] A. Gursoy, N. Karali, *Eur. J. Med. Chem.* **2003**, *38*, 633. https://doi.org/10.1016/S0223-5234(03)00085-0
[15] B. Yiğit, M. Yiğit, P. Taslimi, Y. Gök, İ. Gulçin, *Arch. Pharm.* **2018**, *351*, e1800146. https://doi.org/10.1002/ardp.201800146
[16] M. Rezai, Ç. Bayrak, P. Taslimi, İ. Gulçin, A. Menzek, *Turk. J. Chem.* **2018**, *42*(*3*), 808. https://doi.org/10.3906/kim-1709-34
[17] A. Behcet, T. Çağlılar, D. Barut Celepci, A. Aktaş, P. Taslimi, Y. Gök, M. Aygün, R. Kaya, İ. Gulçin, *J. Mol. Struct.* **2018**, *1170*, 160. https://doi.org/10.1016/j.molstruc.2018.05.077
[18] S. Burmaoglu, A. O. Yilmaz, P. Taslimi, O. Algul, D. Kılıç, İ. Gulçin, *Arch. Pharm.* **2018**, *351*(*2*), e1700314. https://doi.org/10.1002/ardp.201700314
[19] H. I. Gul, E. Mete, P. Taslimi, İ. Gulcin, C. T. Supuran, *J. Enzyme Inhib. Med. Chem.* **2017**, *32*(*1*), 189. https://doi.org/10.1080/14756366.2016.1244533
[20] D. Ozmen Ozgun, C. Yamali, H. İ. Gül, P. Taslimi, İ. Gülçin, T. Yanik, C. T. Supuran, *J. Enzyme Inhib. Med. Chem.* **2016**, *31*(*6*), 1498. https://doi.org/10.3109/14756366.2016.1149479
[21] P. Taslimi, İ. Gulcin, B. Ozgeris, S. Goksu, F. Tumer, S. H. Alwasel, C. T. Supuran, *J. Enzyme Inhib. Med. Chem.* **2016**, *31*(*1*), 152. https://doi.org/10.3109/14756366.2015.1014476
[22] E. Bursal, P. Taslimi, A. C. Gören, İ. Gülçin, *Biocatal. Agric. Biotechnol.* **2020**, *28*, e101711. https://doi.org/10.1016/j.bcab.2020.101711
[23] S. Ökten, A. Aydın, Ü. M. Koçyiğit, O. Çakmak, S. Erkan, C. A. Andac, P. Taslimi, İ. Gülçin, *Arch. Pharm.* **2020**, *353*, e2000086. https://doi.org/10.1002/ardp.202000086
[24] M. Işık, S. Akocak, N. Lolak, P. Taslimi, C. Türkeş, İ. Gülçin, M. Durgun, Ş. Beydemir, *Arch. Pharm.* **2020**, *353*, e2000102. https://doi.org/10.1002/ardp.202000102
[25] H. Genç Bilgiçli, D. Ergön, P. Taslimi, B. Tüzün, İ. Akyazı Kuru, M. Zengin, İ. Gülçin, *Bioorg. Chem.* **2020**, *101*, e103969. https://doi.org/10.1016/j.bioorg.2020.103969
[26] N. Lolak, S. Akocak, C. Türkeş, P. Taslimi, M. Işık, Ş. Beydemir, İ. Gülçin, M. Durgun, *Bioorg. Chem.* **2020**, *100*, e103897. https://doi.org/10.1016/j.bioorg.2020.103897
[27] H. Akıncıoğlu, İ. Gülçin, *Mini Rev. Med. Chem.* **2020**, *20*, 703. https://doi.org/10.2174/1389557520666200103100521
[28] A. Biçer, R. Kaya, G. Yakalı, M. S. Gültekin, G. Turgut Cin, İ. Gülçin, *J. Mol. Struct.* **2019**, *1204*, e127453. https://doi.org/10.1016/j.molstruc.2019.127453
[29] P. Taslimi, E. Köksal, A. C. Gören, E. Bursal, A. Aras, Ö. Kılıç, S. Alwasel, İ. Gülçin, *Arab. J. Chem.* **2020**, *13*, 4528. https://doi.org/10.1016/j.arabjc.2019.10.002
[30] İ. Gülçin, A. C. Gören, P. Taslimi, S. Alwasel, O. Kılıc, E. Bursal. *Biocatal. Agric. Biotechnol.* **2020**, *23*, e101441. https://doi.org/10.1016/j.bcab.2019.101441
[31] A. Aras, E. Bursal, F. Türkan, H. Tohma, Ö. Kılıç, İ. Gülçin, E. Köksal, *Chem. Biodivers.* **2019**, *16*, e1900341. https://doi.org/10.1002/cbdv.201900341
[32] İ. Gülçin, A. Z. Tel, A. C. Gören, P. Taslimi, S. Alwasel, *J. Food Meas. Charact.* **2019**, *13*, 2062. https://doi.org/10.1007/s11694-019-00127-2
[33] N. Öztaşkın, R. Kaya, A. Maraş, E. Şahin, İ. Gülcin, S. Göksu, *Bioorg. Chem.* **2019**, *87*, 91. https://doi.org/10.1016/j.bioorg.2019.03.010
[34] P. Taslimi, İ. Gulçin, *J. Biochem. Mol. Toxicol.* **2017**, *31*(*10*), e21956. https://doi.org/10.1002/jbt.21956
[35] N. Öztaşkın, Y. Çetinkaya, P. Taslimi, S. Göksu, İ. Gülçin, *Bioorg. Chem.* **2015**, *60*, 49. https://doi.org/10.1016/j.bioorg.2015.04.006
[36] C. Yamali, H. İ. Gül, A. Ece, P. Taslimi, İ. Gulçin, *Chem. Biol. Drug Des.* **2018**, *91*(*4*), 854. https://doi.org/10.1111/cbdd.13149
[37] P. Taslimi, C. Caglayan, İ. Gulçin, *J. Biochem. Mol. Toxicol.* **2017**, *31*(*12*), e21995. https://doi.org/10.1002/jbt.21995
[38] P. Taslimi, İ. Gulçin, *J. Food Biochem.* **2018**, *42*(*3*), e12516. https://doi.org/10.1111/jfbc.12516
[39] İ. Gulçin, P. Taslimi, *Expert Opin. Ther. Pat.* **2018**, *28*(*7*), 541. https://doi.org/10.1080/13543776.2018.1487400
[40] M. Zengin, H. Genc, P. Taslimi, A. Kestane, E. Guclu, A. Ogutlu, O. Karabay, İ. Gulçin, *Bioorg. Chem.* **2018**, *81*, 119. https://doi.org/10.1016/j.bioorg.2018.08.003
[41] İ. Gulçin, P. Taslimi, A. Aygün, N. Sadeghian, E. Bastem, O. I. Kufrevioglu, F. Turkan, F. Şen, *Int. J. Biol. Macromol.* **2018**, *119*, 741. https://doi.org/10.1016/j.ijbiomac.2018.08.001
[42] P. Taslimi, H. E. Aslan, Y. Demir, N. Oztaskin, A. Maraş, İ. Gulçin, S. Beydemir, S. Goksu, *Int. J. Biol. Macromol.* **2018**, *119*, 857. https://doi.org/10.1016/j.ijbiomac.2018.08.004
[43] Y. Demir, P. Taslimi, M. S. Özaslan, N. Oztaskin, Y. Çetinkaya, İ. Gulçin, Ş. Beydemir, S. Goksu, *Arch. Pharm.* **2018**, *351*, e1800263. https://doi.org/10.1002/ardp.201800263
[44] C. Çağlayan, Y. Demir, S. Küçükler, P. Taslimi, F. M. Kandemir, İ. Gulçin, *J. Food Biochem.* **2019**, *43*(*2*), e12720. https://doi.org/10.1111/jfbc.12720
[45] M. Miyagawa, H. Kanemasa, S. Nakagawa, T. Nitan, M. Matsumoto, K. Tokita, Y. Kajita, S. Mitsufuji, T. Okanoue, *Gastroenterol. Endosc.* **2006**, *48*, 329.
[46] A. Zubrienė, J. Smirnovienė, A. Smirnov, V. Morkūnaitė, V. Michailovienė, V. Jachno, J. Juozapaitienė, P. Norvaišas, E. Manakova, S. Gražulis, D. Matulis, *Biophys. Chem.* **2015**, *205*, 51. https://doi.org/10.1016/j.bpc.2015.05.009
[47] B. Cornelio, M. Laronze-Cochard, M. Ceruso, M. Ferraroni, G. A. Rance, F. Carta, A. N. Khlobystov, A. Fontana, C. T. Supuran, J. Sapi, *J. Med. Chem.* **2016**, *59*, 721. https://doi.org/10.1021/acs.jmedchem.5b01771
[48] J. D. Cox, J. A. Hunt, K. M. Compher, C. A. Fierke, D. W. Christianson, *Biochemistry* **2000**, *39*, 13687. https://doi.org/10.1021/bi001649j
[49] Y. Ashani, J. Grunwald, C. Kronman, B. Velan, A. Shafferman, *Mol. Pharmacol.* **1994**, *45*, 555.
[50] J. Cheung, E. N. Gary, K. Shiomi, T. L. Rosenberry, *ACS Med. Chem. Lett.* **2013**, *4*, 1091. https://doi.org/10.1021/ml400304w
[51] C. Jang, D. K. Yadav, L. Subedi, R. Venkatesan, A. Venkanna, S. Afzal, E. Lee, J. Yoo, E. Ji, S. Y. Kim, M. Kim, *Sci. Rep.* **2018**, *8*, e14921. https://doi.org/10.1038/s41598-018-33354-6
[52] J. Cheung, M. J. Rudolph, F. Burshteyn, M. S. Cassidy, E. N. Gary, J. Love, M. C. Franklin, J. J. Height, *J. Med. Chem.* **2012**, *55*, 10282. https://doi.org/10.1021/jm300871x
[53] M. Yiğit, B. Yiğit, P. Taslimi, İ. Özdemir, M. Karaman, İ. Gulçin, *J. Mol. Struct.* **2020**, *1207*, e127802. https://doi.org/10.1016/j.molstruc.2020.127802
[54] K. Yamamoto, H. Miyake, M. Kusunoki, S. Osaki, *FEBS J.* **2010**, *277*, 4205. https://doi.org/10.1111/j.1742-4658.2010.07810.x
[55] L. Englert, K. Silber, H. Steuber, S. Brass, B. Over, H. Gerber, A. Heine, W. E. Diederich, G. Klebe, *Med. Chem.* **2010**, *5*, 930. https://doi.org/10.1002/cmdc.201000084
[56] S. G. Davies, K. B. Ling, P. M. Roberts, A. J. Russell, J. E. Thomson, P. A. Woods, *Tetrahedron* **2010**, *66*, 6803. https://doi.org/10.1016/j.tet.2010.06.059
[57] N. N. Smirnova, Y. V. Kozhevnikov, *Deposited Doc* **1982**, *1615-85*, 9.
[58] J. A. Verpoorte, S. Mehta, J. T. Edsall, *J. Biol. Chem.* **1967**, *242*, 4221.
[59] A. Sujayev, E. Garibov, P. Taslimi, İ. Gülçin, S. Gojayeva, V. Farzaliyev, S. H. Alwasel, C. T. Supuran, *J. Enzyme Inhib. Med. Chem.* **2016**, *31*(*6*), 1531. https://doi.org/10.3109/14756366.2016.1156104
[60] B. Turan, K. Sendil, E. Sengul, M. S. Gultekin, P. Taslimi, İ. Gulcin, C. T. Supuran, *J. Enzyme Inhib. Med. Chem.* **2016**, *31*(*S1*), 79. https://doi.org/10.3109/14756366.2016.1170014

[61] F. Özbey, P. Taslimi, İ. Gulcin, A. Maraş, S. Goksu, C. T. Supuran, *J. Enzyme Inhib. Med. Chem.* **2016**, *31*(*S2*), 79.
[62] E. Garibov, P. Taslimi, A. Sujayev, Z. Bingöl, S. Çetinkaya, İ. Gulcin, S. Beydemir, V. Farzaliyev, S. H. Alwasel, C. T. Supuran, *J. Enzyme Inhib. Med. Chem.* **2016**, *31*(*S3*), 1. https://doi.org/10.1080/14756366.2016.1198901
[63] M. M. Bradford, *Anal. Biochem.* **1976**, *72*, 248. https://doi.org/10.1016/0003-2697(76)90527-3
[64] K. Aksu, B. Özgeriş, P. Taslimi, A. Naderi, İ. Gülçin, S. Göksu, *Arch. Pharm.* **2016**, *349*(*12*), 944. https://doi.org/10.1002/ardp.201600183
[65] G. Ellman, K. Courtney, V. Andres, R. Featherston, *Biochem. Pharm.* **1961**, *7*, 88. https://doi.org/10.1016/0006-2952(61)90145-9
[66] U. Atmaca, S. Daryadel, P. Taslimi, M. Çelik, İ. Gülçin, *Arch. Pharm.* **2019**, *352*, e1900200. https://doi.org/10.1002/ardp.201900200
[67] F. Türkan, M. N. Atalar, A. Aras, İ. Gülçin, E. Bursal, *Bioorg. Chem.* **2020**, *94*, e103333. https://doi.org/10.1016/j.bioorg.2019.103333
[68] Y. Tao, Y. Zhang, Y. Cheng, Y. Wang, *Biomed. Chromatogr.* **2013**, *27*, 148. https://doi.org/10.1002/bmc.2761
[69] P. Taslimi, H. Akıncıoğlu, İ. Gulçin, *J. Biochem. Mol. Toxicol.* **2017**, *31*(*11*), e21973. https://doi.org/10.1002/jbt.21973
[70] LigPrep, Schrödinger, LLC, New York, NY, 2020.
[71] K. Turhan, B. Pektaş, F. Türkan, F. T. Tuğcu, Z. Turgut, P. Taslimi, H. S. Karaman, İ. Gulcin, *Arch. Pharm.* **2020**, *353*, e2000030. https://doi.org/10.1002/ardp.202000030
[72] QikProp, Schrödinger, LLC, New York, NY, 2020.
[73] Protein Preparation Wizard; Epik, Schrödinger, LLC, New York, NY, 2016; Impact, Schrödinger, LLC, New York, NY, 2016; Prime, Schrödinger, LLC, New York, NY, 2020.
[74] P. Taslimi, K. Turhan, F. Türkan, H. S. Karaman, Z. Turgut, İ. Gulcin, *Bioorg. Chem.* **2020**, *97*, e103647. https://doi.org/10.1016/j.bioorg.2020.103647
[75] SiteMap, Schrödinger, LLC, New York, NY, 2020.
[76] Induced Fit Docking protocol; Glide, Schrödinger, LLC, New York, NY, 2016; Prime, Schrödinger, LLC, New York, NY, 2020.

SUPPORTING INFORMATION

Additional Supporting Information may be found online in the supporting information tab for this article.

How to cite this article: Tokalı FS, Taslimi P, Demircioğlu İH, et al. Design, synthesis, molecular docking, and some metabolic enzyme inhibition properties of novel quinazolinone derivatives. *Arch Pharm*. 2021;354:e2000455. https://doi.org/10.1002/ardp.202000455